Journal of Chromatography A, 1218 (2011) 2467–2475

Contents lists available at ScienceDirect

Journal of Chromatography A

journal homepage: www.elsevier.com/locate/chroma

Dispersive solid-phase extraction based on oleic acid-coated magnetic nanoparticles followed by gas chromatography–mass spectrometry for UV-filter determination in water samples

Iván P. Román[a], Alberto Chisvert[b,*], Antonio Canals[a,**]

[a] Departamento de Química Analítica, Nutrición y Bromatología e Instituto Universitario de Materiales, Facultad de Ciencias, Universidad de Alicante, P.O. Box 99, E-03080 Alicante, Spain

[b] Departamento de Química Analítica, Facultad de Química, Universidad de Valencia, 46100 Burjassot, Valencia, Spain

ARTICLE INFO

Article history:
Received 20 December 2010
Received in revised form 16 February 2011
Accepted 18 February 2011
Available online 25 February 2011

Keywords:
Dispersive solid-phase extraction
Emerging pollutants
Gas chromatography–mass spectrometry
Magnetic nanoparticles
UV filters
Water analysis

ABSTRACT

A sensitive analytical method to concentrate and determine extensively used UV filters in cosmetic products at (ultra)trace levels in water samples is presented. The method is based on a sample treatment using dispersive solid-phase extraction (dSPE) with laboratory-made chemisorbed oleic acid-coated cobalt ferrite ($CoFe_2O_4$@oleic acid) magnetic nanoparticles (MNPs) as optimized sorbent for the target analytes. The variables involved in dSPE were studied and optimized in terms of sensitivity, and the optimum conditions were: mass of sorbent, 100 mg; donor phase volume, 75 mL; pH, 3; and sodium chloride concentration, 30% (w/v). After dSPE, the MNPs were eluted twice with 1.5 mL of hexane, and then the eluates were evaporated to dryness and reconstituted with 50 μL of N,O-bis(trimethylsilyl)trifluoroacetamide (BSTFA) for the injection into the gas chromatography–mass spectrometry (GC–MS). Under the optimized experimental conditions the method provided good levels of repeatability with relative standard deviations below 16% ($n = 5$, at 100 ng L^{-1} level). Limit of detection values ranged between 0.2 and 6.0 ng L^{-1}, due to the high enrichment factors achieved (i.e., 453–748). Finally, the proposed method was applied to the analysis of water samples of different origin (tap, river and sea). Recovery values showed that the matrices under consideration do not significantly affect the extraction process.

1. Introduction

The UV filters are the active ingredients in sunscreen cosmetic products, used to mitigate or minimize the adverse effects that the deleterious UV solar radiation can cause to human health [1]. These compounds are characterized by possessing a high UV-radiation absorption capacity and not for belonging to the same chemical family. Among them, we can found benzophenones, *p*-aminobenzoic acid and its derivatives, salicylates, cinnamates, camphor derivatives, triazines, benzotriazoles, benzimidazoles and others [1,2]. The specific compounds, their maximum permitted concentrations and conditions of use are regulated by the legislation in force in each country, and can be found elsewhere [1,2].

Nowadays, in order to achieve greater protection to solar radiation, UV filters are added not only to cosmetics for sunbathing but also to other daily cosmetic and personal-care products, such as face day-creams, after-shave products, makeup formulations, lipsticks, shampoos, etc. [2]. Moreover, some of these compounds can also be added as additives to textiles, plastics, paints, car polishes, etc. [3].

Besides this excessive use, potential endocrine disruption and developmental toxicity are attributed to organic UV filters and, accordingly, their monitoring in the aquatic environment has gained special interest in recent years [4]. It should be mentioned that not only do they reach the aquatic environment via indirect routes like other contaminants, but also directly from recreational activities, such as sunbathing and swimming in seas, lakes and rivers. In fact, although the levels found in environmental waters are in the ng L^{-1} range, they are not far below the dose that causes toxic effects in animals [4], and therefore, organic UV filters have recently been classed as emerging pollutants.

Although they are recognized as pollutants, there are no official analytical methods to control them in the aquatic environment. Moreover, taking into account that the maximum residue limits for these emerging pollutants occur at ultra-trace levels, sensitive analytical methods are needed. Different reviews [3,5,6] have reported UV-filter determination in environmental water samples in recent years, thus showing it to be an area of growing interest. Either liquid chromatography (LC) or gas chromatography (GC),

* Corresponding author. Tel.: +34 96 354 49 00; fax: +34 96 354 44 36.
** Corresponding author. Tel.: +34 96 590 97 90; fax: +34 96 590 97 90.
E-mail addresses: alberto.chisvert@uv.es (A. Chisvert), a.canals@ua.es (A. Canals).

0021-9673/$ – see front matter © 2011 Elsevier B.V. All rights reserved.
doi:10.1016/j.chroma.2011.02.047

generally coupled to mass spectrometry (MS) detectors, are the techniques of choice. Furthermore, concentration and/or clean-up techniques are employed in order to improve their sensitivity and limits of detection and/or to eliminate some potentially interfering compounds. As can be seen in the literature, a few papers propose traditional liquid–liquid extraction (LLE) [7] or traditional solid-phase extraction (SPE) [8,9]. However, current trends focus on miniaturization by using microextraction techniques, which consume less toxic organic solvent than the above-mentioned traditional ones (or even avoid them). Thus, solid-phase microextraction (SPME) [10], stir-bar sorptive extraction (SBSE) [11–13], single-drop microextraction (SDME) [14,15], membrane-assisted liquid–liquid extraction (MALLE) [16], dispersive liquid–liquid microextraction (DLLME) [17,18] and cloud point extraction (CPE) [19] have been proposed as microextraction techniques for UV-filter determination in environmental water samples.

Dispersive solid phase extraction (dSPE) [20] is a promising sample pretreatment technique. In dSPE, a SPE sorbent is dispersed in a sample solution containing the target analytes. After extraction, the sorbent containing the retained analytes is settled by centrifugation. This approach enables the sorbent to interact equally with all the sorbent particles, achieving greater capacity per amount of sorbent and avoiding channeling or blocking of cartridges or disks, as occurs in traditional SPE. A modified approach using advesicle solid-phase dispersion has been reported for UV-filter determination in water samples [21].

It should be emphasized that, in recent years, nanomaterials have gained popularity as acceptor phases due to their higher specific surface area (surface area/mass ratio). As in DLLME and CPE, the higher the interfacial area between extractant and sample, the faster the mass transfer, thus equilibrium is reached sooner. Additionally, sorbent phases with magnetic properties enable assisted magnetic separation of the aqueous sample. Based on these two principles, magnetic (or rather superparamagnetic) nanoparticles (MNPs) have been used as extracting phases in water analysis. Briefly, MNPs are added to the sample containing the target compounds, and after stirring they are recovered from the solution by means of a strong magnet, and finally the target compounds are chemically desorbed from the MNPs by means of an appropriate solvent. In this sense, Shen et al. [22] experimentally showed that dispersed MNPs (i.e., dSPE) provided better results than the same sorbent packed in a cartridge (i.e., SPE) for organophosphorus pesticide determination.

Moreover, several surface modifications have been proposed to improve MNPs capacity, such as polymers, surfactants, biological receptors, gold, carbon or silica shells, etc. [23–27]. In case of surfactant-coated MNPs (i.e., hemimicelles), the surfactant can be physisorbed or chemisorbed depending on the nature of the interaction within the surfactant and the nanoparticle. In the former, the surfactant is easily desorbed from the MNP surface during the analyte elution step, whereas the obtained eluate is surfactant-free in the latter [28], owing to the stronger interaction, thus preventing matrix effects in the LC system. For instance, cetyltrimethylammonium bromide (CTAB) or cetylpyridinium chloride (CPC) physisorbed on MNPs were used for dSPE of phenols [29,30], and chlorophenols [31]. On the other hand, Peng et al. [32] used chemisorbed MNPs with a double layer of undecanoic acid to extract 2-nitrophenol and 2-hydroxyphenol. Later on, decanoic acid was also used as a surfactant chemically adsorbed in MNPs to extract four triazine herbicides [33]. More recently, several alkyl carboxylates [28] or *n*-octadecylphosphonic acid [34] chemisorbed on MNPs have also been used for polycyclic aromatic hydrocarbon extraction.

It should be emphasized that despite the high concentrating potential of the different nanomaterials, and the ease of handling MNPs, neither nanomaterial-based nor MNPs-based dSPE have been used to concentrate UV filters. Within this context, the aim of this work was to develop a sensitive analytical method to determine typical UV filters (see Table 1) used in cosmetic products in environmental water samples. The method consists in a MNPs-based dSPE procedure using laboratory-made chemisorbed oleic acid-coated MNPs before GC–MS analysis, which enables the target analytes to be determined in the low ng L^{-1} range.

2. Experimental

2.1. Apparatus

An 800 Series Digital hot plate stirrer from VWR (Darmstadt, Germany) and an UP200S-Stand-Mounted ultrasonic processor from Dr. Hielscher (Teltow, Germany) with 200 W effective power/amplitude output and working frequency of 24 kHz, and with a S_7 titanium sonotrode (7 mm diameter, 100 mm length) were used for MNPs synthesis. A micropH 2002 pH-meter from Crison (Alella, Spain) was used for the pH measurements. A 513 ultrasound bath (50 Hz, 360 W) from J.P. Selecta S.A. (Barcelona, Spain) and a $2X^3$ vortex agitator from Velp Scientific (Milano, Italy) were used to mix the MNPs with the sample. A miVac centrifugal concentrator from Genevac (Ipswich, UK) was used to evaporate the eluates to dryness.

2.2. Reagents, samples and materials

Ethanol and acetic acid LC-grade from Scharlau (Barcelona, Spain) were used for standard preparation and pH adjustment, respectively. Sodium hydroxide and ammonium hydroxyde solution (25% (w/v), $d = 0.91$ g mL^{-1}) reagent-grade used for pH adjustment and MNPs synthesis and sodium chloride used for ionic strength studies were purchased also from Scharlau. Cobalt dichloride hexahydrate ($CoCl_2{\cdot}6H_2O$) from Scharlau, iron trichloride hexahydrate ($FeCl_3{\cdot}6H_2O$), iron dichloride tetrahydrate ($FeCl_2{\cdot}4H_2O$), oleic acid (90%), CTAB (≥98%), polyacrylic acid (PAA) solution (50% (w/w)) and tetraethyl orthosilicate (TEOS) all from Sigma–Aldrich (Steinheim, Germany), and two commercial copolymers of polyethylene oxide and polypropylene oxide amino termined named Jeffamine XTJ-234 (PEO/PPO-NH_2, EO:PO = 6.1:1, $M_w = 300$ g mol^{-1}) and Jeffamine CTJ-507 (PEO/PPO-NH_2, EO:PO = 1:6.5, $M_w = 200$ g mol^{-1}) from Huntsman Corp. (Houston, TX, USA), were used in the synthesis of MNPs.

2-Ethylhexyl salicylate (ES) (99%), 2-ethylhexyl 4-dimethylaminobenzoate (ethylhexyl dimethyl PABA (EDP)) (99.8%), 2-hydroxy-4-methoxybenzophenone (benzophenone-3 (BZ3)) (98%) and 2-ethylhexyl 4-methoxycinnamate (EMC) (99.8%) from Sigma–Aldrich, 3,3,5-trimethylciclohexyl salicylate (homosalate (HS)) (>98%) from Merck (Darmstadt, Germany), isoamyl 4-methoxycinnamate (IMC) (99.3%) from Haarmann and Reimer (Parets del Vallés, Spain), 3-(4′-methylbenzylidene)camphor (MBC) (99.7%) from Guinama S.L. (Valencia, Spain), and 2-ethylhexyl 2-cyano-3,3-diphenylacrylate (octocrylene, (OCR)) (>98%) from F. Hoffmann-La Roche Ltd. (Basel, Switzerland) were used as standards. Standard stock solutions of each UV filter (5000 mg L^{-1}) were prepared in ethanol. Multicomponent working standard solutions were freshly prepared daily by proper dilution of the ethanolic standard stock solutions with de-ionized water. Hexachlorobencene (99%) also from Sigma–Aldrich was used as internal standard.

All the aqueous solutions used in the synthesis of MNPs were prepared using ultra-pure water (resistivity ≥18 MΩ cm) obtained by a NANOpure II system from Barnstead (Boston, MA, USA).

Table 1
Name, abbreviation and chemical structure of the target analytes. The retention time, the time windows and the selected ions employed in the GC–MS analysis are also shown.

Name	Abbreviation	Chemical structure	Retention time (min)	Time window (min)	Selected ions (m/z)[d]
2-Ethylhexyl salicylate	ES	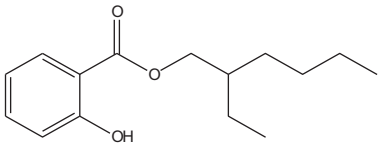	22.3[c]	22.0–25.7	**195**, 307[c]
3,3,5-Trimethylciclohexyl salicylate *(homosalate)*	HS[a]	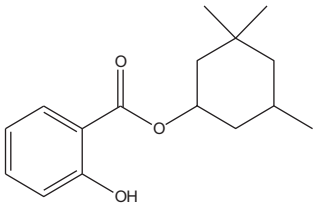	23.6 (HS_1)[c] 25.0 (HS_2)[c]	22.0–25-7 (HS_1, HS_2)	**195**, 319[c]
Isoamyl 4-methoxycinnamate	IMC[b]	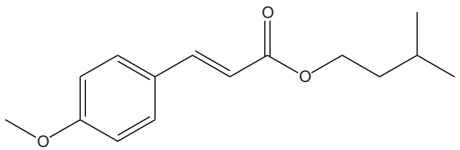	21.5 (*Z*), 26.4 (*E*)	18.0–22.0 (*Z*) 25.7–28.3 (*E*)	161, **178**, 248
3-(4′-Methylbenzylidene)camphor	MBC[b]	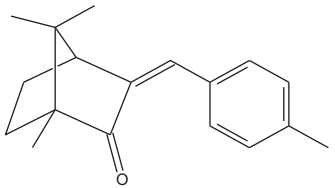	26.3 (*Z*), 26.9 (*E*)	22.0–28.3 (*Z*, *E*)	128, 211, **254**
2-Hydroxy-4-methoxybenzophenone *(benzophenone-3)*	BZ3	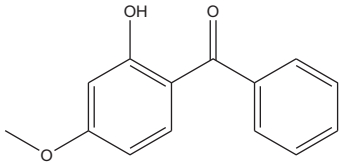	27.3[c]	25.7–28.3	**285**, 300[c]
2-Ethylhexyl 4-methoxycinnamate	EMC[b]	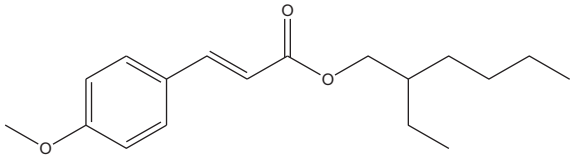	29.1 (*Z*), 31.5 (*E*)	28.3–33.0 (*Z*, *E*)	161, **178**, 290

Table 1 (*Continued*)

Name	Abbreviation	Chemical structure	Retention time (min)	Time window (min)	Selected ions (*m/z*)[d]
2-Ethylhexyl 4-dimethylaminobenzoate *(ethylhexyl dimethyl PABA)*	EDP		30.8	28.3–33.0	148, **165**, 277
2-Ethylhexyl 2-cyano-3,3-diphenylacrylate *(octocrylene)*	OCR		35.0	33.0–40.0	**204**, 232, 360

[a] There are two positional isomers (HS_1 and HS_2).
[b] The commercial *E* isomer experiments isomerisation to the *Z* isomer when exposed to light.
[c] These values are for the silylated forms, which are obtained by derivatization with BSTFA for the GC–MS analysis.
[d] Quantitation ion is shown in bold.

N,O-bis-(trimethylsilyl)trifluoroacetamide (containing 1% (v/v) trimethylchlorosylane) (BSTFA) also from Sigma–Aldrich was used as derivatization reagent for GC analysis.

Ultra high purity helium from Carburos Metálicos S.A. (Paterna, Spain) was used as carrier gas in the GC–MS system. Ultra high purity argon and nitrogen from Air Liquide S.A. (Alicante, Spain) were used in the synthesis of MNPs.

The real sample set consists of a tap water from Burjassot (Valencia, Spain), a river water from the Turia River (Valencia, Spain) and a sea water from Postiguet Beach (Alicante, Spain). Water samples were collected in 1 L topaz glass bottles, and stored in the dark at 4 °C until their analysis.

2.3. Synthesis of MNPs

MNPs were synthesized according to the procedures described below. After each synthesis all the MNPs were separated by a magnet and washed several times with ultrapure water and ethanol for removing the synthesis by-products, especially physisorbed surfactants that could remain when surfactants are involved in the synthesis of MNPs [28].

2.3.1. Magnetite and cobalt ferrite coated with PEO/PPO-PAA nanoparticles (Fe_3O_4@PEO/PPO-PAA and $CoFe_2O_4$@PEO/PPO-PAA)

The synthesis procedure followed for the preparation of Fe_3O_4@PEO/PPO-PAA MNPs was previously described by Moeser et al. [35]. Briefly, it consists of two steps: the synthesis of a copolymer graft and the coprecipitation of magnetite in aqueous medium containing the copolymer. The copolymer graft was produced by heating, at 180 °C for 2 h under a nitrogen blanket, a mixture of 0.46 g of Jeffamine XTJ-234, 0.31 g of Jeffamine XTJ-507 and 3.09 g of 50% PAA. After that, the copolymer was dissolved in deoxygenated water to produce a 33% (w/v) solution. The magnetite nanoparticles were synthesized in 37.5 mL of water containing 2.35 g of $FeCl_3{\cdot}6H_2O$, 0.86 g of $FeCl_2{\cdot}4H_2O$ and 3.75 g of the 33% (w/v) graft copolymer solution. The mixture was stirred vigorously for 30 min with a hot plate magnetic stirrer purging with nitrogen and then heated to 80 °C. When the temperature was reached, the nitrogen flow was stopped and 5 mL of ammonium hydroxyde (ca. 13 M) was added and stirred 30 min more at 80 °C. Similarly, $CoFe_2O_4$@PEO/PPO-PAA MNPs were synthesized using the same reaction conditions but employing 1.08 g of $CoCl_2{\cdot}6H_2O$ instead of $FeCl_2{\cdot}4H_2O$.

2.3.2. Cobalt ferrite coated with oleic acid nanoparticles ($CoFe_2O_4$@oleic acid)

A modified procedure was used for the synthesis of $CoFe_2O_4$@oleic acid MNPs based on that prepared by Maaz et al. [36]. Basically 125 mL of 0.4 M $FeCl_3$ solution and 125 mL of 0.2 M $CoCl_2$ solution were mixed with a magnetic stirrer. Then 125 mL of 3 M sodium hydroxyde solution were added dropwise. Finally, 10 mL of oleic acid were added and the reaction mixture was heated to 80 °C for 1 h.

2.3.3. Uncoated cobalt ferrite nanoparticles ($CoFe_2O_4$)

A similar procedure as described in Section 2.3.2 was used but using CTAB instead of oleic acid as a surfactant. In this case, 7.8 g of CTAB were added and the reaction mixture was heated to 80 °C for 1 h. After that, MNPs were rinsed with ethanol for removing CTAB.

2.3.4. Cobalt ferrite coated with silica shell nanoparticles ($CoFe_2O_4$@SiO_2)

These MNPs were synthesized using the procedure described in Section 2.3.2 but without adding oleic acid. As soon as the MNPs were separated and washed, they were dispersed in 450 mL of ethanol using the ultrasound processor (the pulse and the

amplitude was set for all the synthesis process at 100% and 80%, respectively) and purging the solution with argon to remove dissolved oxygen. The silica shell was formed following an adapted procedure from Morel et al. [37]. Briefly, a chilled solution of 10.5 mL of ammonia in 140 mL of ultrapure water was added to the colloidal dispersion. The mixture was sonicated 15 min, and after that, a chilled solution of 20 g of TEOS in 75 mL of ethanol was added in the base of the sonotrode with a pipette. After 30 min, the argon flow and the ultrasound energy were stopped and the particles were separated.

2.4. Instruments for MNPs characterization

Different instruments for MNPs characterization were used (see Supplementary material).

2.5. MNPs-based dSPE proposed procedure

An aliquot of 75 mL of aqueous sample or standard solution, adjusted to pH 3 and to 30% (w/v) NaCl, was placed in a 100-mL glass bottle, and then 100 mg of $CoFe_2O_4$@oleic acid MNPs were added. The bottle was placed in an ultrasound bath for 2 min and stirred with a vortex agitator for 2 min at 40 Hz (maximum setting speed). After that, the bottle was placed over a strong Fe-Nd-B magnet (magnetization N45, 45 mm diameter and 30 mm thickness) from Supermagnete (Uster, Switzerland) for 1 min. The solution was decanted and separated from the MNPs with the magnet on the base or walls of the bottle. Then, UV filters were eluted twice from the MNPs with 1.5 mL of hexane (2 min in ultrasonic bath followed by 2 min with vortex agitation). Finally, both hexane eluates were merged and evaporated to dryness by using a centrifugal concentrator under vacuum at room temperature, and the residue was dissolved in 50 μL of BSTFA. After that, 10 μL of internal standard solution (1 mg L^{-1} of hexachlorobenzene in hexane) were added. The final solution was placed in a 200 μL-insert, which was inserted in a 1.5 mL-vial for GC–MS analysis.

2.6. GC–MS analysis

A Focus GC gas chromatograph coupled to a DSQII mass spectrometric detector (operated in positive electron ionization mode at ionization energy of 70 eV, with a multiplier voltage set at 1400 V) and an AI 3000 autosampler, was purchased from Thermo Fisher Scientific (Austin, TX, USA). 2 μL of the aforementioned derivatized solutions were injected into the GC injection port set at 280 °C in splitless mode (splitless time 1 min), and run at 1 mL min^{-1} helium constant flow rate by using a TR-5MS capillary column (30 m length × 0.25 mm I.D., 0.25 μm film thickness) also purchased from Thermo Fisher Scientific. The oven temperature program was: from 70 °C (1 min) ramped at 10 °C min^{-1} to 170 °C (10 min), then ramped at 2 °C min^{-1} to 200 °C and finally ramped at 10 °C min^{-1} to 280 °C (6 min). The transfer line and the ion source temperatures were 280 and 300 °C, respectively. The chromatograms were recorded in the selected ion monitoring (SIM) mode. The analytes were measured at the time windows and the mass/charge (m/z) ratios shown in Table 1. In the case of hexachlorobenzene (internal standard) m/z 142, m/z 249 and m/z 284 (from 16.0 to 18.0 min) were used. The m/z ratios of un-silylated ES, HS_1, HS_2 and BZ3 (used in preliminary studies) were m/z 120, m/z 138 and m/z 250 for ES (from 17.5 to 19.5 min); m/z 120, m/z 138 and m/z 262 for HS_1 and HS_2 (from 19.5 to 22.0 min); and m/z 151, m/z 227 and m/z 228 for BZ3 (from 28.1 to 32.0 min). The quantitation ion is shown in bold.

Note that some UV filters exist in the environment as geometrical isomers (E/Z) due to the presence of an exocyclic C=C double bond adjacent to the aromatic ring. Commercial substances are mainly E isomers and isomerize to the Z form upon exposure to the UV radiation [5,38]. The rate of isomerization depends on the compound, spectrum of light source and matrix (solvent). In environmental samples, isomerization of E-IMC, E-MBC and E-EMC occurs, so for quantitative purposes the detection response is assumed to be the same for both and summed up since only the E-isomers were available as standards [38].

The ratio of the peak area of each target analyte to that of the internal standard (A_i/A_{IS}) was used to construct the corresponding calibration curves.

The enrichment factor (EF) was calculated as $EF = C_{ext,i}/C_{0,i}$, where $C_{ext,i}$ is the concentration of the i-target analyte in the final BSTFA solution (obtained by external calibration with standards in BSTFA) and $C_{0,i}$ is the initial concentration of this compound in the aqueous phase (obtained by using a BSTFA standard solution of the same concentration, since water cannot be injected into the GC–MS).

3. Results and discussion

In order to obtain MNPs with a suitable sorbent for the extraction of the target lipophilic UV filters, Fe_3O_4@PEO/PPO-PAA MNPs were selected as a starting point. The bifunctional polymer layer was comprised of an outer hydrophilic poly(ethylene oxide) (PEO) region for colloidal stability, and an inner hydrophobic poly(propylene oxide) (PPO) region for solubilization of organic compounds. However, the poor oxidative stability of magnetite (Fe_3O_4) is a drawback, mainly at low pH values. In this sense, cobalt ferrite ($CoFe_2O_4$) coated-MNPs were also synthesized, owing to their excellent chemical stability, good chemical hardness and also the ability to control crystal size within the superparamagnetic and single domain limits [36,39–41]. On the other hand, additional stabilization can be achieved by growing a silica shell over the ferrite MNPs [30,37,42]. Among the different procedures reported for this purpose, an ultrasound assisted procedure was selected and adapted in this work, due to its faster synthesis and control of shell thickness; but cobalt ferrite was used instead of magnetite.

Therefore, different kinds of MNPs were synthesized and further tested for UV-filter extraction in terms of the analytical signal (i.e., ratio of the peak area of each target analyte to that of the internal standard (A_i/A_{IS}), which was used to calculate the EF). Once the best-suited type of MNPs was selected, these MNPs were characterized. Finally, the experimental variables involved in the dSPE procedure were optimized. Nevertheless, it should be pointed out that, during the optimization experiments, hydroxylated UV filters (i.e., ES, HS and BZ3) gradually deteriorated in tailing peaks from run to run, thus redounding in bad repeatability. This was especially problematic in case of BZ3, which was excluded in the optimization experiments. Nevertheless, as discussed later (see Section 3.4), a derivatization step using a silylating agent was finally carried out to overcome this drawback and enable the determination of BZ3.

3.1. Effect of the MNP type

Different kinds of MNPs were evaluated for the extraction and concentration of typical lipophilic organic UV filters. Apart from the extraction efficiency of MNPs other features were considered, such as sedimentation speed or chemical inertness. The MNPs evaluated were: Fe_3O_4@PEO/PPO-PAA, $CoFe_2O_4$@PEO/PPO-PAA, $CoFe_2O_4$@oleic acid, uncoated $CoFe_2O_4$ and $CoFe_2O_4$@SiO_2. The effect of MNPs type on the EF is depicted in Fig. 1 (results for uncoated $CoFe_2O_4$ are not shown as extraction was not successful). As expected, for all target analytes the highest EF values were obtained with $CoFe_2O_4$@oleic acid MNPs, as the lipophilic coating of these MNPs is highly attractant to lipophilic organic UV filters. Moreover, it should be pointed out that these MNPs boast

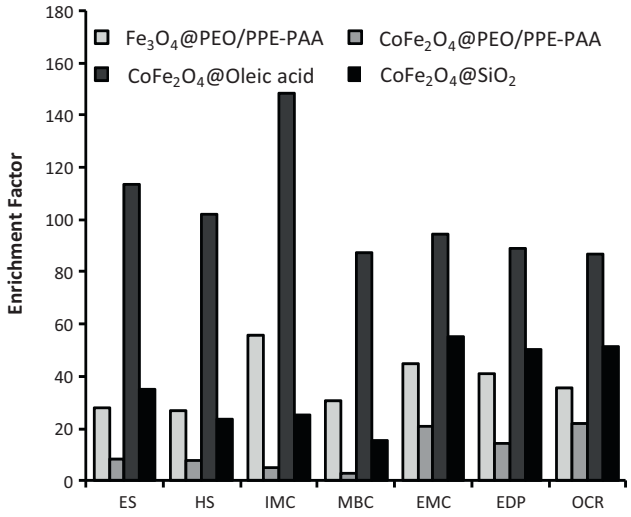

Fig. 1. Effect of the MNP type on the enrichment factor (other extraction conditions: 100 mg of MNPs, 10 mL of the aqueous donor phase, without salt addition and pH 6). Results are the average of 2 replicates.

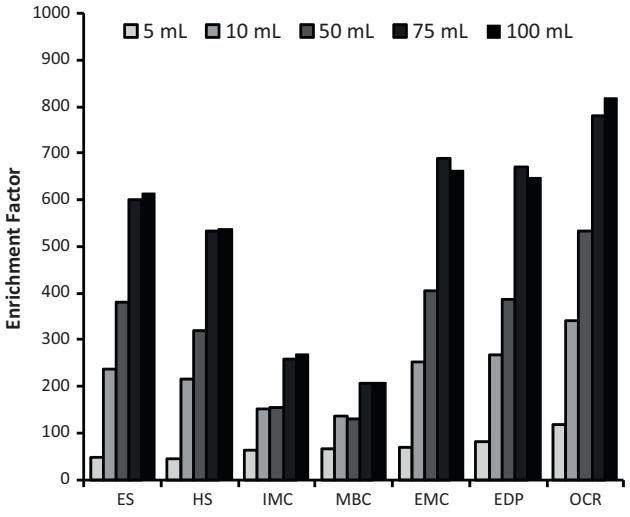

Fig. 2. Effect of the volume of the aqueous donor phase on the enrichment factor (other extraction conditions: 100 mg of $CoFe_2O_4$@oleic acid, without salt addition and pH 6). Results are the average of 2 replicates.

good chemical inertness. Then, different amounts (100, 200 and 300 mg) of $CoFe_2O_4$@oleic acid MNPs were evaluated. The EFs were not improved from 100 to 300 mg, thus 100 mg was employed for further experiments.

3.2. Characterization of the $CoFe_2O_4$@oleic acid MNPs

Characterization techniques were applied to confirm the nanosize and porosity, the magnetic properties and the surface modification of the selected MNPs. In summary, the results demonstrated that particles with 5–20 nm size coated with chemisorbed oleic acid were obtained, showing a mesoporous structure (BET surface area of 97.3 $m^2\,g^{-1}$, micropore volume of 0.033 $cm^3\,g^{-1}$ and mesopore volume of 0.245 $cm^3\,g^{-1}$) and superparamagnetic properties (saturation magnetization of 59.4 emu g^{-1}) (see Supplementary material).

3.3. Study of the experimental variables involved in the dSPE procedure

Several variables may affect the extraction process with dispersed MNPs, such as volume, ionic strength and pH of the donor aqueous solution. Thus, the influence of all these variables was evaluated in terms of EF. In this sense, an aqueous standard solution containing the target UV filters at 100 ng L^{-1} was used to perform the optimization experiments in the MNPs-based dSPE procedure.

On the other hand, acetone, ethanol and hexane were studied for the elution of UV filters from the MNPs. Results (not shown) revealed that poor elution efficiency (thus redounding in lower EF) was obtained on using acetone, whereas similar results were obtained with ethanol and hexane. However, when ethanol was used, the retained water in the MNPs was removed and mixed with this solvent, and thus the time required for evaporation to dryness increased considerably unless an additional drying step (e.g., by using a nitrogen stream) of the MNPs was performed. However, when hexane was used, water was easily separated by means of a pipette owing to its non-miscibility. Therefore, hexane was used as elution solvent since it reduced the time in the evaporation step and avoided an additional step for drying the MNPs. An additional experiment was carried out in order to study the elution volume to desorb the analytes from the MNPs. Thus, the hexane volume was varied from 1 to 2 mL, and the best conditions were found when eluting twice with 1.5 mL of hexane.

Moreover, to avoid the possible adsorption of UV filters on the walls of the flask, solvent was added to the donor solution, since the influence of this parameter has been reported important when these compounds were extracted by SBSE [11]. Different amounts of ethanol were tested (i.e., no solvent addition, 1 and 5% (v/v)), finding that lower EFs were attained when ethanol was added. This was attributed to the fact that the solvent favors the solubility of the analytes in the donor solution. Hence, no organic solvent was added for further experiments.

3.3.1. Effect of the volume of the donor aqueous phase

It is well known that increasing the volume of the donor phase increases the total mass of analytes available for extraction, and thus EFs are increased, and method sensitivity is improved. The effect of donor phase volume was examined by extracting different volumes (10–100 mL) of aqueous standard solutions (100 ng L^{-1}) (Fig. 2). Although similar EFs were obtained for 75 and 100 mL of sample volume, the former was chosen since the extraction efficiency was higher.

3.3.2. Effect of the ionic strength of the donor aqueous phase

The ionic strength might not only affect the extraction efficiency (and thus the EF) of the target compounds, but also the stability of the MNPs colloidal suspension and the settling speed.

Currently, there is considerable research into the stability and spatial organization (structure) of colloidal particles. In diluted dispersions (such as in the present study), the origin and nature of interparticle forces and how they affect the coagulation are key to colloid stability. A detailed understanding of Van der Waals and electrostatic forces is an essential issue in colloid coagulation. Furthermore, thermodynamically unstable colloids can be kinetically stable depending on the surface charges or potentials. The backbone of the classical theory of electrostatic stability of colloids, known as the Derjaguin–Landau–Verwey–Overbeek (DLVO) theory, is based on kinetic arguments. The equilibrium state is forecasted by thermodynamics; however, kinetics often determines whether the equilibrium state will be reached and how fast. It should be mentioned that among all the variables affecting the trend of the net interaction potential curve, none is as accessible to empirical adjustment as the electrolyte concentration [43]. This effect depends on both the electrolyte concentration and charge. As the electrolyte concentration increases, the stability of the colloidal suspension decreases, owing to the shorter distance from which

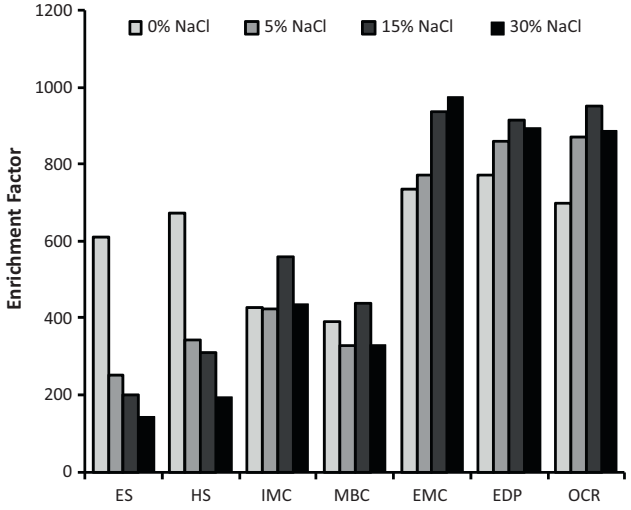

Fig. 3. Effect of the ionic strength of the aqueous donor phase on the enrichment factor (other extraction conditions: 100 mg of $CoFe_2O_4$@oleic acid, 75 mL of the aqueous donor phase and pH 6). Results are the average of 2 replicates.

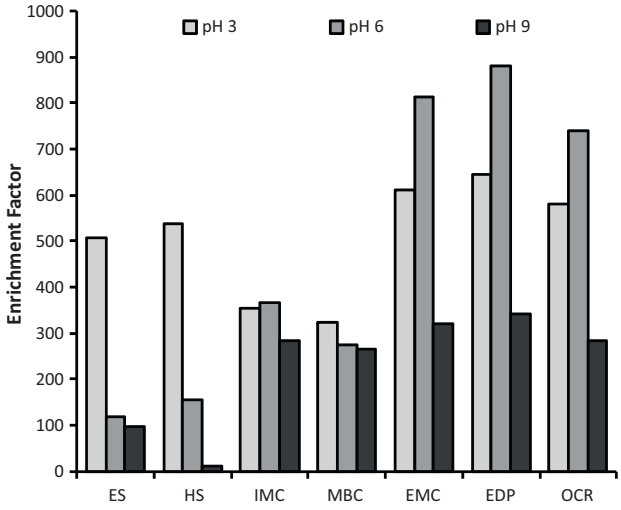

Fig. 4. Effect of the pH of the aqueous donor phase on the enrichment factor (other extraction conditions: 100 mg of $CoFe_2O_4$@oleic acid, 75 mL of the aqueous donor phase and 30% w/v NaCl). Results are the average of 2 replicates.

the interparticle repulsion decreases. The DLVO theory provides a quantitative explanation for this effect that causes a lyophobic colloid to undergo coagulation. For a particular salt, there is a defined concentration beyond which coagulation is induced, called critical coagulation concentration (CCC). The time required for the dispersed colloid to settle is used to determine this CCC. However, the CCC was not determined because salt content in sea water (about 30–330 g L^{-1}) is by far beyond this CCC for NaCl.

In the present study, when salt was added the time required for MNPs settling was observed to reduce sharply (from about 10 min without salt addition to less than 1 min for 30% (w/v) NaCl). Apart from this improvement, it is noteworthy that when salt was added (30%) MNPs were quantitatively settled, whereas without salt addition MNPs settling was not quantitative and clear solutions were not achieved.

Regarding the target UV-filter extraction, two behavioral patterns were observed: for potentially ionizable analytes (i.e., ES, HS) EF decreased with salt addition, meanwhile EF increased for all the rest (Fig. 3). Due to this, 30% (w/v) NaCl was selected because EFs improved for most of the analytes and the ionizable UV filters could be enhanced by selecting a suitable pH value.

3.3.3. Effect of the pH of the donor aqueous phase

As mentioned above, some target UV filters are potentially ionizable compounds. Taking into account the lipophilic phase of the MNPs surface, the neutral (i.e., not ionized) forms of the compounds are expected to be easily extracted. In this sense, pH values ranging from 3 to 9 were studied (lower pH values were not tested in order to avoid the ionization of EDP). As can be seen in Fig. 4 the EFs for HS and ES were considerably improved at pH 3, which was in accordance with previously reported studies [10]. Therefore, a pH value of 3 was selected for further experiments.

3.4. Derivatization reaction

Finally, as mentioned above, hydroxylated UV filters (i.e., ES, HS and BZ3) exhibited peak tailing as the number of GC injections increased. This occurs because the column bleeding, and thus the unbounded silica surface, increases with the use of the column, which redoundes in a stronger interaction within siloxane and hydroxylated UV filters. Therefore, a derivatization step prior to the GC injection was considered in order to convert the hydroxylated UV filters into more inert homologues by means of derivatization of the –OH moiety.

Silylation is by far the most commonly used derivatization reaction for compounds containing labile hydrogens, which are replaced by alkylsilyl moieties, usually trimethylsilyl. BSTFA was found to be the best silylation reagent for hydroxylated UV-filters [17,44].

Additionally, the use of silylating reagents is an approach reported to solve the difficulties related to introducing a surfactant-rich phase in GC [45]: (1) mainly the surfactants can be absorbed onto the stationary phase and alter its polarity, thus causing important retention times to shift during subsequent injections; (2) the surfactant itself and/or degradation by-products can also elute as a series of peaks over a period of time from the column, that overlaps or obscures the analyte peak; (3) a surfactant-rich phase could

Table 2
Main analytical features of the proposed MNPs-based dSPE-GC–MS method for target UV-filter determination in water samples.

Analyte	EF	Slope × 10^{-3} (ng L^{-1})$^{-1}$ [a,b]	Intercept × $^{-2}$ [a,b]	r^2 [b]	Repeatability [c] RSD (%)	LODs (ng L^{-1})	LOQs (ng L^{-1})
ES	609	2.9 ± 0.3	−8 ± 14	0.990	10.4	0.2	0.5
HS	539	2.98 ± 0.17	−18 ± 11	0.997	13.9	0.4	1.5
IMC	453	1.66 ± 0.04	−0.8 ± 1.5	0.9990	15.0	6.0	20.0
MBC	495	0.579 ± 0.015	−1.2 ± 0.7	0.9990	12.6	5.8	19.3
BZ3	748	5.3 ± 0.3	−21 ± 15	0.995	5.6	0.2	0.8
EDP	592	1.59 ± 0.03	−1.0 ± 1.6	0.9991	16.0	3.1	10.2
EMC	659	0.466 ± 0.018	1.6 ± 0.9	0.998	8.8	2.5	8.3
OCR	568	4.98 ± 0.07	−0.4 ± 0.4	0.9998	7.9	1.8	5.9

[a] Value ± standard deviation.
[b] Working range: 20–1000 ng L^{-1}. Number of calibration points: 6.
[c] Five replicate analysis of an aqueous standard solution containing 100 ng L^{-1} of the target analytes.

Table 3
UV-filter contents in three environmental water samples and their recovery values obtained by applying the proposed MNPs-based dSPE-GC–MS method.

Analyte	Sea water			Tap water			River water		
	Initial found amount ($ng\,L^{-1}$)[a,b]	Found amount after spiking ($ng\,L^{-1}$)[a,c]	Recovery (%)[a,c]	Initial found amount ($ng\,L^{-1}$)[a,b]	Found amount after spiking ($ng\,L^{-1}$)[a,c]	Recovery (%)[a,c]	Initial found amount ($ng\,L^{-1}$)[a,b]	Found amount after spiking ($ng\,L^{-1}$)[a,c]	Recovery (%)[a,c]
ES	792 (14)	1222 (1)	86 (14)	160 (8)	615 (11)	91 (14)	146 (13)	586 (3)	88 (13)
HS	625 (9)	1030 (11)	81 (14)	<LOD	515 (11)	103 (11)	342 (6)	712 (4)	74 (7)
IMC	245 (3)	645 (5)	80 (6)	65 (12)	315 (7)	63 (14)	<LOD	595 (11)	119 (11)
MBC	358 (8)	758 (6)	80 (10)	<LOQ	505 (1)	101 (1)	264 (11)	794 (9)	106 (14)
BZ3	254 (4)	879 (12)	125 (13)	<LOQ	450 (11)	90 (11)	428 (8)	993 (15)	113 (17)
EMC	409 (2)	774 (16)	73 (16)	126 (12)	621 (6)	99 (13)	56 (7)	531 (4)	95 (8)
EDP	682 (3)	1187 (14)	101 (14)	<LOD	430 (21)	86 (21)	240 (15)	770 (10)	106 (18)
OCR	<LOQ	440 (21)	88 (21)	<LOQ	550 (3)	110 (3)	<LOD	440 (2)	88 (2)

[a] $n = 3$, %RSD (%) within parentheses.
[b] <LOD: below limit of detection; <LOQ: detected but below limit of quantification.
[c] Spiked with $500\,ng\,L^{-1}$.

clog the GC column; and (4) surfactants can increase the dirtiness of the MS ion source. Hence, the derivatization step was performed for two reasons: the derivatization of hydroxylated target analytes and the derivatization of undesired molecules of oleic acid, which could be released from the MNPs surface.

3.5. Analytical figures of merit of the proposed MNPs-based dSPE-GC–MS method

Quality features of the proposed MNPs-based dSPE-GC–MS method were evaluated under the final optimized conditions. The achieved EFs ranged from 453 to 748 depending on the analyte (Table 2).

The employed working range was set from $20\,ng\,L^{-1}$ to $1000\,ng\,L^{-1}$ with good correlation coefficients. Table 1 shows the equations of the calibration lines obtained with standard aqueous solutions of all the target analytes extracted by the proposed procedure. The limits of detection (LODs) and limits of quantification (LOQs) were calculated using the 3-fold and 10-fold, respectively, signal-to-noise ratio (S/N) criteria. LODs and LOQs of the target UV filters, also shown in Table 2, are in the low $ng\,L^{-1}$ level. The repeatability, expressed as relative standard deviation (RSD), was evaluated by applying the proposed method to five replicate standard aqueous solutions containing the target analytes at $100\,ng\,L^{-1}$. Results reveal that acceptable precision was achieved for all the target analytes (Table 2).

3.6. Analysis of environmental water samples

In order to assess the suitability of the developed MNPs-based dSPE-GC–MS method for the analysis of real samples, three different surface water samples of different matrix composition (tap, river and sea) collected in the summer of 2009 (see Section 2.2) were analyzed (Table 3).

To perform recovery studies, and thus evaluate matrix effects, the three water samples were spiked with the target analytes at $500\,ng\,L^{-1}$. The relative recoveries, defined as the amount found in spiked samples using standards subjected to the same extraction procedure as samples, are also shown in Table 3. The results demonstrate that the matrices under consideration do not significantly affect the extraction process.

4. Conclusions

The chemisorbed oleic acid-coated cobalt ferrite ($CoFe_2O_4$@oleic acid) MNPs constitute a good alternative to physisorbed surfactant-coated magnetite MNPs, since oleic acid presents a stronger interaction with the MNP surface, and cobalt ferrite affords additional chemical stability compared with magnetite-based MNPs. Higher oxidative stability and wider pH applicability ranges are advantageous inertness properties reported in this study. Moreover, chemisorbed oleic acid provides a more surfactant-free eluate than physisorbed surfactants. Additionally, the use of BSTFA avoids possible problems linked to the GC–MS system if any surfactant molecules are released from the MNPs surface.

On the basis of the results obtained in this study about UV-filter determination in real water samples, we conclude that $CoFe_2O_4$@oleic acid MNPs perform dSPE efficiently, with high enrichment factors (ranging from 453 to 748), providing LODs within the low $ng\,L^{-1}$ range. Dispersive solid-phase extraction, therefore, is performed by a simple, rapid, matrix-independent method at the low levels required for these emerging pollutants. No additional clean-up steps are required, thus dSPE saves time, labor, money and solvent use compared with the tiresome traditional SPE. Furthermore, low extraction times are needed in MNPs-based dSPE,

since the mass transfer between sample and extractant is quickly achieved due to the higher area of the nanomaterials and the MNPs are easily recovered by means of a magnet.

Acknowledgements

Financial support from the Spanish Government (Projects PET2006-706-00, CTQ2008-06730-C02-01 and >CTQ2009-12709) and the Regional Government of Valencia (Spain) (Projects ACOMP/2009/144, ACOMP2010/047 and A-04/09) is gratefully acknowledged. Authors thank to Huntsman Corp. for the donation of Jeffamine XTJ-234 and Jeffamine CTJ-507. Authors also thank Dr. Ana Silver from the Department of Inorganic Chemistry of University of Alicante for her assistance in the determination of the nitrogen adsorption isotherm. I.P.R. also thanks "Caja de Ahorros del Mediterraneo (CAM)" for his predoctoral grant and "Xarxa d'Universitats Lluís Vives" for the DRAC mobility grant. This work is part of the Doctoral Thesis of Iván P. Román.

Appendix A. Supplementary material

Supplementary material associated with this article can be found, in the online version, at doi:10.1016/j.chroma.2011.02.047.

References

[1] A. Salvador, A. Chisvert, in: A. Salvador, A. Chisvert (Eds.), Analysis of Cosmetic Products, Elsevier, Amsterdam, 2007, p. 83.
[2] A. Salvador, A. Chisvert, Anal. Chim. Acta 537 (2005) 1.
[3] D.L. Giokas, A. Salvador, A. Chisvert, Trends Anal. Chem. 26 (2007) 360.
[4] S.D. Richardson, Anal. Chem. 81 (2009) 4645.
[5] M. Silvia Díaz-Cruz, M. Llorca, D. Barceló, Trends Anal. Chem. 27 (2008) 873.
[6] S.D. Richardson, Anal. Chem. 82 (2010) 4742.
[7] H.K. Jeon, Y. Chung, J.C. Ryu, J. Chromatogr. A 1131 (2006) 192.
[8] P. Cuderman, E. Heath, Anal. Bioanal. Chem. 387 (2007) 1343.
[9] R. Rodil, J.B. Quintana, P. López-Mahia, S. Muniategui-Lorenzo, D. Prada-Rodríguez, Anal. Chem. 80 (2008) 1307.
[10] N. Negreira, I. Rodríguez, M. Ramil, E. Rubí, R. Cela, Anal. Chim. Acta 638 (2009) 36.
[11] R. Rodil, M. Moeder, J. Chromatogr. A 1179 (2008) 81.
[12] M. Kawaguchi, R. Ito, H. Honda, N. Endo, N. Okanouchi, K. Saito, Y. Seto, H. Nakazawa, J. Chromatogr. A 1200 (2008) 260.
[13] M. Haunschmidt, C.W. Klampfl, W. Buchberger, R. Hertsens, Anal. Bioanal. Chem. 397 (2010) 269.
[14] L. Vidal, A. Chisvert, A. Canals, A. Salvador, Talanta 81 (2010) 549.
[15] N. Okanouchi, H. Honda, R. Ito, M. Kawaguchi, K. Saito, H. Nakazawa, Anal. Sci. 24 (2008) 627.
[16] R. Rodil, S. Schrader, M. Moeder, J. Chromatogr. A 1216 (2009) 4887.
[17] I. Tarazona, A. Chisvert, Z. León, A. Salvador, J. Chromatogr. A 1217 (2010) 4771.
[18] N. Negreira, I. Rodríguez, E. Rubí, R. Cela, Anal. Bioanal. Chem. 398 (2010) 995.
[19] D.L. Giokas, V.A. Sakkas, T.A. Albanis, D.A. Lampropoulou, J. Chromatogr. A 1077 (2005) 19.
[20] M. Anastassiades, S.J. Lehotay, D. Stajnbaher, F.J. Schenck, J. AOAC Int. 86 (2003) 412.
[21] N.A. Parisis, D.L. Giokas, A.G. Vlessidis, N.P. Evmiridis, J. Chromatogr. A 1097 (2005) 17.
[22] H.-Y. Shen, Y. Zhu, X.-E. Wen, Y.-M. Zhuang, Anal. Bioanal. Chem. 387 (2007) 2227.
[23] D. Horák, M. Babic, H. Macková, M.J. Benes, J. Sep. Sci. 30 (2007) 1751.
[24] K. Aguilar-Arteaga, J.A. Rodríguez, E. Barrado, Anal. Chim. Acta 674 (2010) 157.
[25] A.S. de Dios, M.E. Díaz-García, Anal. Chim. Acta 666 (2010) 1.
[26] W. Schärtl, Nanoscale 2 (2010) 829.
[27] L. Bai, B. Mei, Q.Z. Guo, Z.G. Shi, Y.Q. Feng, J. Chromatogr. A 1217 (2010) 7331.
[28] A. Ballesteros-Gómez, S. Rubio, Anal. Chem. 81 (2009) 9012.
[29] X. Zhao, Y. Shi, Y. Cai, S. Mou, Environ. Sci. Technol. 42 (2008) 1201.
[30] X. Zhao, Y. Shi, T. Wang, Y. Cai, G. Jiang, J. Chromatogr. A 1188 (2008) 140.
[31] J. Li, X. Zhao, Y. Shi, Y. Cai, S. Mou, G. Jiang, J. Chromatogr. A 1180 (2008) 24.
[32] Z. Peng, K. Hidajat, M.S. Uddin, Korean J. Chem. Eng. 20 (2003) 896.
[33] Y. Song, S. Zhao, P. Tchounwou, Y.M. Liu, J. Chromatogr. A 1166 (2007) 79.
[34] J. Ding, Q. Gao, D. Luo, Z.G. Shi, Y.Q. Feng, J. Chromatogr. A 1217 (2010) 7351.
[35] G.D. Moeser, K.A. Roach, W.H. Green, P.E. Laibinis, T.A. Hatton, Ind. Eng. Chem. Res. 41 (2002) 4739.
[36] K. Maaz, A. Mumtaz, S.K. Hasanain, A. Ceylan, J. Magn. Magn. Mater. 308 (2007) 289.
[37] A.L. Morel, S.I. Nikitenko, K. Gionnet, A. Wattiaux, J. Lai-Kee-Him, C. Labrugere, B. Chevalier, G. Deleris, C. Petibois, A. Brisson, M. Simonoff, Nano 2 (2008) 847.
[38] T. Poiger, H.R. Buser, M.E. Balmer, P.A. Bergqvist, M.D. Müller, Chemosphere 55 (2004) 951.
[39] Y. Cedeño-Mattei, O. Perales-Perez, M.S. Tomar, F. Roman, P.M. Voyles, W.G. Stratton, J. Appl. Phys. 103 (2008).
[40] M.A.G. Soler, E.C.D. Lima, S.W. da Silva, T.F.O. Melo, A.C.M. Pimenta, J.P. Sinnecker, R.B. Azevedo, V.K. Garg, A.C. Oliveira, M.A. Novak, P.C. Morais, Langmuir 23 (2007) 9611.
[41] D.S. Mathew, R.S. Juang, Chem. Eng. J. 129 (2007) 51.
[42] C.R. Vestal, Z.J. Zhang, Nano Lett. 3 (2003) 1739.
[43] P.C. Hiemenz, R. Rajagopalan, in: P.C. Hiemenz, R. Rajagopalan (Eds.), Principles of Colloid and Surface Chemistry, New York, 1997, p. 525.
[44] K.W. Ro, J.B. Choi, M.H. Lee, J.W. Kirn, J. Chromatogr. A 688 (1994) 375.
[45] Y. Takagai, W.L. Hinze, Anal. Chem. 81 (2009) 7113.